

Dispersion measurement method with down conversion process

Marta Misiaszek ^{†,1}, Andrzej Gajewski ^{†,1} and Piotr Kolenderski ¹

¹*Faculty of Physics, Astronomy and Informatics,
Nicolaus Copernicus University, Grudziadzka 5, 87-100 Toruń, Poland**

Proper characterization of nonlinear crystals is essential for designing single photon sources. We show a technique for dispersion characterization of a nonlinear material by making use of phase matching in the process of parametric down conversion. Our method is demonstrated on an exemplary periodically poled potassium titanyl phosphate KTiOPO_4 crystal phase-matched for 396 nm to 532 nm and 1550 nm. We show a procedure to characterize the dispersion in the range of 390 to 1800 nm by means of only one spectrometer for the UV-visible range.

Single photon sources are essential for experimental implementations of various quantum information processing and communication protocols. One of the most popular types of such sources is based on the process of spontaneous parametric down-conversion (SPDC). The process takes place in a nonlinear medium where a photon of a pump beam decays into a pair of photons. Technically, information about dispersion in a crystal is the prerequisite for the design and fabrication of such a source. There are many crystals that allow for efficient pair generation. Consequently, there is a plethora of possibilities for the manipulation of photon states [1, 2]. Those properties are defined by crystal and pump characteristics, of which dispersion is the most important.

Dispersion is described by a tensor of rank two composed of electrical permittivities. After diagonalization, which is related to a respective rotation of the coordinate system, its diagonal elements are interpreted as refractive indexes [3–5]. The related axes are traditionally called principal axes. Typically, crystals used for photon pair generation are uniaxial or biaxial, which means that the dispersion relation is described by two or three (respectively) independent elements of refractive index tensor. It results in a direction and polarization dependent velocity. This, in turn, is the basis for phase matching in nonlinear processes such as: spontaneous parametric down conversion, second harmonic generation (SHG), sum frequency generation (SFG) etc.

The dispersion relation in a medium can be derived from first principles assuming a simple harmonic oscillator model. The resulting formulas are traditionally called the Sellmeier equations [6]. The form of the original equations was modified over time in order to better conform to experimental observations. Typically, the measurement technique which allows to determine the respective coefficients of the equations is based on a technique resorting to the process of SHG or SFG [3]. It was used for characterization of nonlinear crystals i. e. : LiInS_2 [7], BaGa_4Se_7 [8], $\text{GaS}_x\text{Se}_{1-x}$ [9, 10], LiGaSe_2 [11] etc.

In this letter we show a technique which is based on the nonlinear process of SPDC. Our method can be applied to various types of crystals assuming a phase matching characterization method is available [12–14]. It allows

to determine the coefficients of the Sellmeier equations even with limited detection spectral range. We demonstrate our method experimentally using a periodically poled KTiOPO_4 (PPKTP) crystal. The dispersion and temperature dependence for this crystal were analyzed before in Refs. [15, 17–20]. Our crystal is phase matched for 396 nm to 532 nm + 1550 nm and can be tuned with temperature and pump wavelength. Using only one spectrometer for the range of 340-680 nm, we show a procedure to determine the dispersion in the infrared range.

The pair production rate in the SPDC process depends on the effective nonlinearity of a medium and phase matching conditions [5, 21]. Here, we use a reference frame of the principal axis of the crystal where the collinear propagation is along the x-axis. In general, the direction which results from the collinear phase matching condition does not coincide with the direction for which the effective nonlinearity is the largest. In order to achieve efficient photon generation, crystals are periodically poled, which means that crystal's consecutive domains have the same absolute value of effective nonlinearity, but of opposite sign [22]. These leads to a quasi-phase matching (QPM) equation, which takes the form:

$$\Delta\vec{k} = \vec{k}_P - \vec{k}_{\text{VIS}} - \vec{k}_{\text{IR}} - \frac{2\pi}{\Lambda}\hat{x} = \vec{0}, \quad (1)$$

where Λ is a poling period of a crystal and $\vec{k}_P, \vec{k}_{\text{VIS}}, \vec{k}_{\text{IR}}$ are wavevectors of the pump, visible (VIS) and infrared (IR) photons, respectively. The momentum of a photon in a given mode is proportional to the effective refractive index, which involves, in general, all three indexes of refraction. The dispersion formula for each of the elements is given by the Sellmeier equations [23]:

$$n_j^2(\lambda) = a_{j0} + \frac{a_{j1}}{\lambda^2 - a_{j2}} + \frac{a_{j3}}{\lambda^2 - a_{j4}}, \quad j = x, y, z, \quad (2)$$

where a_{ji} are the Sellmeier coefficients. This form of the Sellmeier equation can be found in i.e. Ref. [15]. In our case the pump photon propagates along the x-axis and its polarization is along the z-axis. The VIS and IR photons are slow polarized and their wavevectors create very small opening angle with wavevector of the pump

photon. Consequently, the dispersion in our example is determined by fifteen coefficients.

In order to calculate a central wavelength of outgoing photons, one needs to solve quasi-phase matching problem given in (1) for photons inside a crystal. It can split into two separate equations – one for wavevector components along the x-axis and one for perpendicular ones [5]:

$$\begin{aligned} n_{\text{VIS}} \frac{\omega_{\text{VIS}}}{\omega_{\text{IR}}} \sin(\theta_{\text{VIS}}) &= n_{\text{IR}} \sin(\theta_{\text{IR}}), \\ n_{\text{VIS}} \frac{\omega_{\text{VIS}}}{\omega_{\text{IR}}} \cos(\theta_{\text{VIS}}) &= n_p \frac{\omega_p}{\omega_{\text{IR}}} - n_{\text{IR}} \cos(\theta_{\text{IR}}) - \frac{2\pi}{\Lambda}, \end{aligned} \quad (3)$$

where θ_{IR} and θ_{VIS} are angles created by wavevectors of IR and VIS photon with x-axis. These angles are defined inside the crystal and they relate to angles outside the medium by Snell's law. The analytical formula for IR photon angle θ_{IR} can be derived from (3). In general, the VIS photon wavelength,

$$\lambda_{\text{VIS}} = \lambda_{\text{VIS}}(\omega_p, \Theta_p, \phi_p, \Theta_{\text{VIS}}, \phi_{\text{VIS}}, T, \Lambda_0, \vec{S}), \quad (4)$$

is a function of the pump photon frequency ω_p , angles of incidence of the pump photon wavevector with the surface of the crystal, Θ_p, ϕ_p , the position of the detector, $\Theta_{\text{VIS}}, \phi_{\text{VIS}}$, the temperature, T , the vector of the fifteen Sellmeier coefficients \vec{S} , and the length of periodic poling Λ_0 . This function can be only solved numerically. In our model the angular frequency of the pump photon ω_p is an argument for the algorithm and the wavelength of VIS photon is a returned value. Our method works in the following way. The wavevectors, polarizations and wavelengths of pump and VIS photons are known from the experiment and Sellmeier coefficients can be easily found in the literature [15, 17–20]. The IR photon wavelength is determined by the pump and VIS photons wavelengths, because the three of them obey energy conservation relation. In order to numerically solve equations we used *Wolfram Mathematica 11* software and its built-in function, *FindRoot*. Method of finding a solution was set to Newton's method. All the arguments of the λ_{VIS} function (4) are assumed to be constant, with the exception of the angular frequency of the pump, ω_p . In Fig. 2 the solid red line shows the numerical solution of (4) for our experimental setup settings using the Sellmeier coefficients from Ref. [15]. The experimental results are marked with green dots.

The experimental setup, depicted in Fig. 1, consists of two parts – the second harmonic generation setup (SHG) and the SPDC source. A tunable femtosecond laser beam is frequency doubled in bismuth triborate (BiB_3O_6) nonlinear crystal. A pair of dichroic mirrors DM1 separates the SHG and the laser beam. The frequency doubled beam is used to pump the PPKTP crystal, with a $4.01\mu\text{m}$ poling period placed on a custom made mount T, which allows to control its temperature and position. The crystal temperature is kept constant at 304.8 K. The VIS

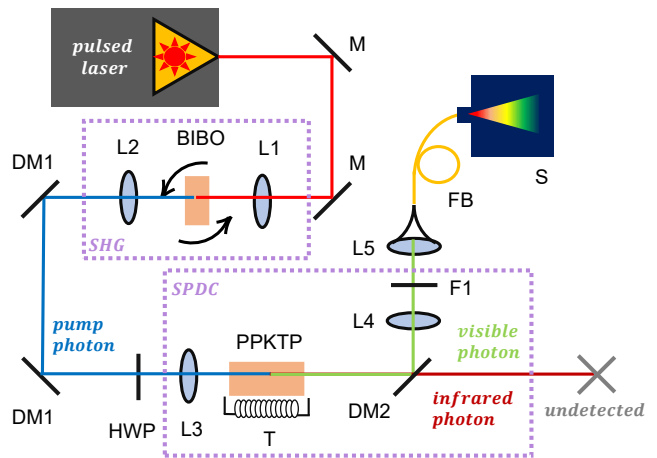


FIG. 1: Experimental setup consists of: the pumping pulsed Ti:Sapphire laser, M – mirror, L1, L2 – lens (focal length $f = 7.5$ cm), BIBO – bismuth triborate crystal, DM1 – dichroic mirror (Semrock T425 LPXR), HWP – half-wave plate, L3, L4 – plano-convex lens ($f = 10$ cm, 12 cm), PPKTP – periodically poled potassium titanyl phosphate crystal, T – temperature controller, DM2 – dichroic mirror (Semrock 76-875 LP), F1 – set of filters (Chroma ET500, Z532-rcd), L5 – aspheric lens ($f = 1.51$ cm), FB – fiber (Thorlabs SMF460B), S – spectrometer (Ocean Optics USB2000+).

photon of generated pair is in the spectral range of 500 to 570 nm and IR photon 1300 to 1900 nm. Next, the beam is split by dichroic mirror DM2, which transmits IR photons while reflecting the VIS and pump photons. Further, a set of filters, F1, reflect the pump photons and transmits the VIS photons. The VIS photons are coupled into a fiber, whereas the IR photons remain undetected.

The measurement procedure is as follows: the femtosecond laser beam is set between 784 nm and 806 nm, which results in a pump photon wavelength in the range 392 nm to 403 nm. For each laser wavelength setting, the spectra of the VIS and the pump photons are measured using a spectrometer. The inset in Fig. 2 presents an example spectra for a pump photon wavelength setting. Next, by fitting gaussian functions, the central wavelengths of both pump and VIS photons are obtained. The results are depicted in Fig. 2 using green dots.

The discrepancy between the experiment and analytical predictions is easy to see. This result was the motivation for further numerical analysis, namely: the computation of Sellmeier coefficients. The goal was to obtain coefficients which would describe more precisely the dispersion in PPKTP crystal in the spectral range of the pump, VIS and IR photons, which is approximately from 390 nm to 1800 nm. We don't want to significantly change the value of dispersion for longer wavelengths. In order to do that we fit the Sellmeier coefficients in the model given in (1) to our experimental data. We reduce the computational effort of numerical optimization by making a few observations. In our case, the dispersion depends

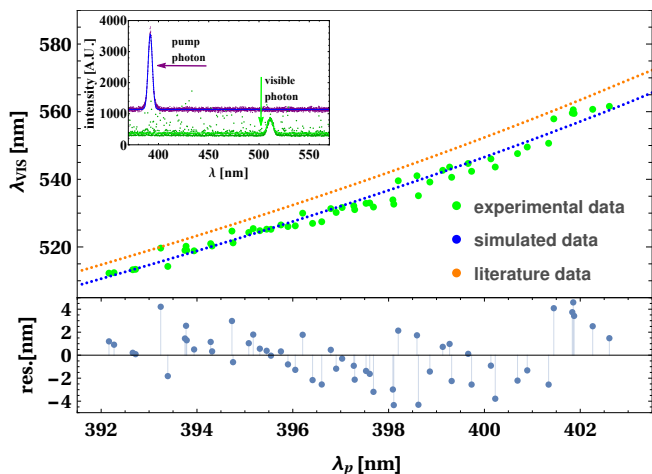


FIG. 2: Experimental results of a visible photon wavelength dependence on the pump wavelength. Inset: an exemplary measurement of a visible photon and pump photon spectra.

predominantly on one element of a tensor, namely n_z . It is because of type 0 configuration, where all the photons have the same polarization and which is close to the collinear propagation. The values of the respective coefficients can be found in Tab. I and Ref. [15]. The Sellmeier equations consist of a constant term and two resonant ones. These resonances correspond to $\sqrt{a_{z3}} = 218$ nm and $\sqrt{a_{z5}} = 9280$ nm, so only the first one is significant for our spectral range. Therefore, in our calculations, we fit only first three coefficients a_{z0}, a_{z1}, a_{z2} . The literature values [15] are the starting point for our optimization procedure.

In order to qualitatively compare Sellmeier equations with the literature (L) and our computed (C) coefficients, we calculate the residual sum of squares (RSS) in the following way:

$$RSS^j = \sum_{i=1}^{N=55} (\lambda_{VIS}^i - \lambda_{VIS}(\omega_P^i; a_{z1}^j, a_{z2}^j, a_{z3}^j; \vec{C}))^2, \quad (5)$$

$$j = L, C,$$

where λ_{VIS}^i are the measured central wavelengths, which are depicted in Fig. 2, and \vec{C} is a vector composed of all the model parameters with Sellmeier coefficients included, which we keep fixed: $\Theta_P = \frac{\pi}{2}$, $\Phi_P = 0$, $\Theta_{VIS} = 0.01237$, $\Phi_{VIS} = 0$, $T = 304.86K$, $\Lambda_0 = 4.01\mu m$ (in 298K).

In the first step we tested the validity of our model by comparing its outcomes with prediction of SNLO [16] software for collinear SPDC. It uses the Sellmeier coefficients from Ref. [15]. We got a perfect agreement. In the next step we used our model to generate a test data with random Gaussian noise up to 5%. Then we used another built in function, NonLinearModelFit (NLF), with conjugate gradient method to estimate Sellmeier coefficients

	a_{z0}	a_{z1} [μm^2]	a_{z2} [μm^2]	a_{z3} [μm^2]	a_{z4} [μm^2]	RSS [nm^2]
liter.	4.59423	0.06206	0.04763	110.807	86.122	1910
comp.	4.59423	0.06272	0.04814	—	—	257
uncer.	0.00015	0.0004	4.5×10^{-6}	—	—	—

TABLE I: Comparison of the literature Ref. [15] and calculated Sellmeier coefficients as in (2)

for the test data. The NLMF numerically looks for values of parameters that minimize RSS , which quantify the quality of each individual fit. For 55 data points, NLMF was able to retrieve parameters with very high accuracy. These computations were also performed multiple times. At this point we established that our method works and can be trusted to compute Sellmeier coefficients which would best fit our data.

For the experimental data set of 55 measurements, the NLMF starts from the initial Sellmeier coefficients, which we take from the Ref. [15]. Next, it computes new parameters for the next step and evaluates new RSS value. The procedure stops when the specified accuracy is reached. We repeated that step 1000 times and achieved the same result every time. That proves the stability of the NLMF algorithm. We proceed with computation of the Sellmeier coefficients for the experimental data. We repeated that step 1000 times to be certain of determinism of our method. The variances of coefficients were below 2.1×10^{-3} %.

The experimental, literature and simulated results are shown in Fig. 2. The comparison of calculated effective refractive index and literature one is presented in Fig. 3. Despite the differences being tiny, as seen in the inset of Fig. 3, change in photon wavelengths is significant. The residual sum of squares of fit for literature effective refractive index is equal to $RSS^L = 1910$ nm², whereas for our computed one it is $RSS^C = 257$ nm². Those values correspond to an average error of approximately 5.9 nm and 2.2 nm, respectively. We used that average error as a measurement error for each data point. As a result NLMF returned parameters with estimated uncertainties. The values and uncertainties of the computed parameters are shown in Tab. I.

Summarizing, the presented method of obtaining Sellmeier coefficient is very accurate. Our method was demonstrated for a PPKTP crystal, for which we got the value differing by 113 standard deviations from the initial one. The method can be used for any other. Moreover the same approach can be used for computation of thermal coefficients i.e. ones describing change of refractive index with temperature. We ran such simulations for n_z , using model and thermal coefficients from the same article as before Ref. [15]. We fitted two out of four parameters to 349 data points. As a result we achieved

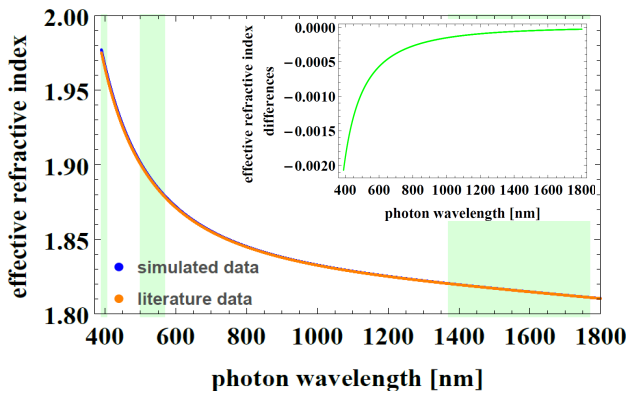


FIG. 3: Effective refractive index. The shaded areas depict the wavelength range accessible by our method in our experiment. Inset: differences between literature and simulated data.

fit with slightly smaller RSS : $2.39579 \times 10^3 \text{ nm}^2$ versus $2.39612 \times 10^3 \text{ nm}^2$, which corresponds to 2.6201 nm and 2.6202 nm, respectively. Such small difference stems from 16% change of non-dispersive term in equation describing change of n_z with the temperature. Further analysis is required in order to investigate a phase matching dependence on the remaining system parameters.

There is also another way to fully utilize our method. In presented work we measured first order quasi phase matching, which led to obtaining very accurate data about Sellmeier coefficients which dominate dispersion in visible range. Measuring higher order quasi phase matching might lead to obtaining additional information about dispersion in crystal, allowing for wider characterization. Our calculation with new set of Sellmeier coefficients implicates that for the same setup we should be able to observe second order quasi phase matching. In our setup, the visible photons with wavelength varying from 428 nm to 439 nm for pump wavelength range 390 nm to 400 nm should be exiting the crystal at opening angle $\Theta_{VIS} = 9$ degree. These wavelengths imply that infrared photon wavelength should be ranging from around 4378 nm to 4485 nm. This quasi phase matching would not only depend on all five Sellmeier coefficient describing n_z but also, because of larger angle, would carry same information about other parameters.

Funding. Foundation for Polish Science (FNP) (project First Team co-financed by the European Union under the European Regional Development Fund, project Homing Plus grant no. 2013-7/9); Ministry of Science and higher Education, Poland (MNiSW) (grant no. 6576/IA/SP/2016, grant no. IP2014 020873); National Science Center, Poland (NCN) (Sonata 12 grant

no. 2016/23/D/ST2/02064)

Acknowledgement. The authors thank Marcin Bober, Mateusz Borkowski, Roman Ciurylo, Michal Zawada for insightful discussions and National Laboratory of Atomic, Molecular and Optical Physics, Torun, Poland for a support.

[†] These authors contributed equally to this work.

* Electronic address: kolenderski@fizyka.umk.pl

- [1] F. Laudenbach, R.-B. Jin, C. Greganti, M. Hentschel, P. Walther, and H. Hubel, *Phys. Rev. Applied* **8**, 024035 (2017).
- [2] P. Kolenderski, W. Wasilewski, and K. Banaszek, *Phys. Rev. A* **80**, 013811 (2009).
- [3] B. E. A. Saleh and M. C. Teich, *Fundamentals of Photonics* (John Wiley & Sons, INC, 2007).
- [4] E. Hecht, *Optics* (Addison Wesley Publishing Company, 2002).
- [5] N. Boeuf, D. Branning, I. Chaperot, E. Dauler, S. Guerin, G. Jaeger, A. Muller, and A. L. Migdall, *Opt. Eng.* **39**, 1016 (2000).
- [6] D. Marcuse, *Principles of Quantum Electronics* (Academic Press, 1980).
- [7] K. Kato and N. Umemura, *Appl Opt* **53**, 7998 (2014).
- [8] K. Kato, K. Miyata, and V. Petrov, *Appl. Opt.* **56**, 2978 (2017).
- [9] K. Kato and T. Mikami, *Appl. Opt.* **53**, 2177 (2014).
- [10] E. Takaoka and K. Kato, *Jpn. J. Appl. Phys.* **38**, 2755 (1999).
- [11] K. Miyata, V. Petrov, and K. Kato, *Appl. Opt.* **56**, 6126 (2017).
- [12] R. Akbari and A. Major, *Laser Phys.* **23**, 035401 (2013).
- [13] C. Schmidt, J. Buhler, A.-C. Heinrich, A. Leitenstorfer, and D. Brida, *J. Opt.* **17**, 094003 (2015).
- [14] R. Riedel, J. Rothhardt, K. Beil, B. Gronloh, A. Klenke, H. Hoppner, M. Schulz, U. Teubner, C. Krankel, J. Limpert, and et al., *Opt. Express* **22**, 17607 (2014).
- [15] K. Kato and E. Takaoka, *Appl. Opt.* **41**, 5040 (2002).
- [16] <http://www.as-photonics.com/snlo>
- [17] S. Manjooan, H. Zhao, I. T. Lima, and A. Major, *Laser Phys.* **22**, 1325 (2012).
- [18] E. Stoumbou, I. Stavarakas, G. Hloupis, A. Alexandridis, D. Triantis, and K. Moutzouris, *Opt. Quantum. Electron.* **45**, 837 (2013).
- [19] H. J. Lee, H. Kim, M. Cha, and H. S. Moon, *Appl. Phys. B* **108**, 585 (2012).
- [20] H. Zhao, I. T. Lima, Jr., and A. Major, *Proc. SPIE* **7750**, 77501D (2010).
- [21] W. H. Louisell, A. Yariv, and A. E. Siegman, *Phys. Rev.* **124**, 1646 (1961).
- [22] M. M. Fejer, G. A. Magel, D. H. Jundt, and R. L. Byer, *IEEE J. Quantum. Electron.* **28**, 2631 (1992).
- [23] D. Marcuse, *Light Transmission Optics* (Van Nostrand Reinhold, 1982), 2nd ed.